UDC 536.421.1; 622.245.5(088.8)

A STUDY OF HEAT TRANSFER GENERALIZATION FOR A COOLING SYSTEM WITH MINERAL MEDIA COATINGS

Genbach A.A., Bondartsev D.Yu.

Almaty University of Power Engineering and Telecommunications named after G. Daukeev, Almaty, Kazakhstan
Corresponding author: d.bondartsev@aues.kz

Abstract. *Studies of heat transfer in cooling systems with natural material coatings have been carried out. The phenomenon of flame spin detonation was observed at an oxidizer excess ratio below unity, with the spraying process being intensified up to sixfold. The coatings demonstrated high reliability compared to other accelerated systems. The maximum specific heat fluxes on the coating range from 2 to 20×10^6 W/m², with oscillation frequencies reaching 200 Hz. The overheating range of the coating was (20–75) K. The granulometric composition of the materials was obtained, and the hydrodynamic operating modes of the burners were selected. A model was developed for the interaction of a supersonic detonation gas jet of the thermal tool acting normally to the coating. The experimentally determined heat transfer coefficients were found to be 5–6 times higher than those predicted by laminar theory, and several times lower than those predicted by turbulent heat transfer laws. The particle flight time, powder diameter, as well as the ultimate compressive and tensile stresses of the coating were determined. The main practical application of the research is thermal protection through cooling with natural coatings (quartzites, granites, teschenites, marbles, tuffs) for highly forced and high-intensity structures in the fields of energy, metallurgy, and mechanical engineering. The primary industrial implementation of the research is the use of a thermal tool for spraying, processing of rocks, drilling, and cutting of reinforced concrete structures during modernization and reconstruction of enterprises.*

Keywords: heat and mass transfer, coatings, thermal tools, combustion chamber, nozzles, detonation torch.

1. Introduction

In recent decades, the problem of protection against high temperatures has become increasingly important, especially in the context of the development of aviation, space technology, energy and other industries where exposure to extreme temperatures is inevitable. In the context of these technological processes, it is necessary to use materials that not only effectively protect against overheating, but also have high resilience, durability and environmental friendliness. The main difference of the performed work is the focus on natural mineral coatings such as quartzites [1], granites [2-3], tuffs [4] and marbles [5] in the context of creating porous cooling systems [6]. The authors consider not only well-known technologies, but also propose innovative solutions based on the application of supersonic detonation jets for sputtering.

One of the main equipment in both power and heat engineering is turbine units – steam [7] or gas turbines [8]. Today, the task of improving the efficiency of combined energy production [9], as well as cooling the turbine combustion chamber using various coolants to increase the coefficient of performance (CoP) of machines and cycles [10–11], remains relevant. The works [12-14] consider heat transfer in homogeneous and inhomogeneous coatings, in special wicks to increase the extraction *q*. Many authors describe studies of the influence of porous coating parameters such as thickness [15-17], porosity and size of

particles from which the structure is made [18], geometry of the structure [19] on boiling processes. There are studies on the influence of external conditions on the boiling intensity, system pressure [20] and surface orientation [21-22], including studies of special coatings of different designs. However, all the listed papers [1-5, 10-22] do not consider the action of capillary and mass forces (ΔP_g, ΔP_{g+cap}), and there is no connection between the bubble dynamics and the boiling curve in a porous medium. Combined cooling systems including powder spraying and capillary-porous structures with fluid boiling, including the use of jet methods of coolant supply with boiling on the cooling (heating) surface, that is, taking into account the speed and underheating of the flow, are not considered.

We introduce cooling elements for various thermal power units (choice of geometry and material of apparatuses, supply and type of energy). The application area of the new system is presented [23], which requires further research of new cooling systems with coatings made of natural materials.

2. Experimental study of the process of application of coatings by spraying

Burners for spraying natural materials have supersonic spin detonation jets [24]. Further development of powder spraying processes is required to create cooling of combustion chambers and increase the efficiency of the elements. Special design of supersonic nozzles with shortened diffuser part is used to carry out detonation mode of thermal tool operation. The cooling system of burners is very effective and allows increasing the resource of combustion chambers (from 100-150 to 500-600 hours).

2.1. Coating spraying tool (see Fig. 1) allows for fire spraying by supersonic detonation high-temperature jet. The powder was mineral particles (granite). The coatings were applied to the metal surface at temperatures up to 2500-3500 ^{0}C and flow velocity up to 2500 m/s.
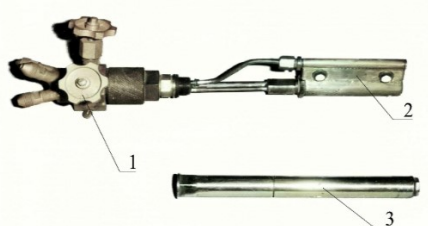
Fig.1. Unit for 1 an automated line. The combustion chamber is cooled by coatings 2 (granite); 3 – housing.

2.2. Conditions for conducting the experiment. A burner power supply circuit was assembled for conducting an experiment with a thermal tool (see Fig. 2): 1 – collector; 2 – pressure gauge; 3 – collector shut-off valve; 4 – oxygen intake shut-off valve; 5 – ramp reducer; 6 – oxygen cylinder; 7 – air cylinder; 8 – manifold pressure regulator; 9 – three-way valve; 10 – shut-off valve, 11 – water sump; 12 – water hose; 13 – air cylinder; 14 – kerosene cylinder; 15 – shut-off valve; 16 – kerosene sump; 17 – kerosene hose; 18 – plug; 19 – thermal tool; 20 – oxygen hose; 21, 25 – shut-off valves and command reducers; 22, 26 – check valves, 23, 27 – filters; 24 – reactive hose.
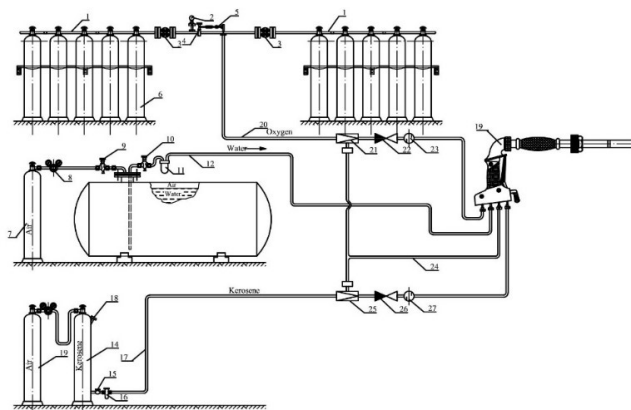
Fig.2. Displacing power supply circuit of thermal tool.

The heat flows q of the burner jet was measured by a sensor made of a copper cylinder, to which the heat flow of the burner jet is connected from one end, and from the other – the end of the cylinder is cooled by a heat pipe. Side surface of the cylinder is thermally insulated with ceramics based on zirconium dioxide. Two chromel-alumel thermocouples are placed in the cylinder. The cylinder was attached to a stationary cooled barrier (coating) having an area larger than the jet braking spot area and cooled by a heat pipe. To determine the specific heat flows q on the jet axis and in the braking spot (on the coating) along the radius r, the flow rate G, pressure P and temperature T of the cooler were measured in order to consolidate the heat balance. Flow rate, fuel and cooler pressure, and in-chamber pressure were also measured [23].

2.3. Samples of natural materials

The sample materials are made of natural mineral media, shown in Fig. 3. Stresses and deformations in the samples were studied, and three copper spirals were used as an energy source. The specific heat fluxes were $(0.25 \div 4.2) \times 10^6$ W/m^2.

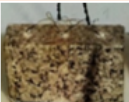| Natural material	Type of material	Hole size, m	Drilling depth, m	Material features
Granite Sample №1		6×10^{-3}	12×10^{-3}	Crystalline rock formed from magma inside the earth's crust. It has characteristic large crystals and has high strength and resistance to wear.
Granite Sample №2		6×10^{-3}	12×10^{-3}	
Tuff Sample №3		6×10^{-3}	12×10^{-3}	Porous rock formed from sediments that contain small fragments of rocks and minerals. Light and porous.
Tuff Sample №4		6×10^{-3}	12×10^{-3}	
Marble Sample №5		6×10^{-3}	12×10^{-3}	Metamorphic rock formed from limestone under the influence of high pressure and temperature. It has characteristic patterns and textures.

Fig.3. Natural materials

3. Results of the experiment in application of coatings by spraying

Fig. 4 shows the structure of the jet flowing from a rocket-type burner (thermal tool). The phenomenon of spin detonation of a supersonic high-temperature multiphase jet has been recorded. The jet is designed for spraying a coating on a metal substrate with the strongest mineral media (powders of granite).


Fig.4. Jet outflow from the nozzle of a thermal tool (see Fig. 1) for spraying:
1 – strong flame swelling due to spin detonation of a supersonic high-temperature jet.

The flame is of an original shape, strongly inflated. The excess oxidant ratio is $\alpha < 1$, the oxidant is additionally applied to the barrier and intensifies the particle spraying process by 2-6 times. The particles in powder form come from the hopper, ejected by a jet. The phenomenon of spin detonation of a supersonic high-temperature jet is presented in Fig. 5. The structure of the flooded jet is recorded.
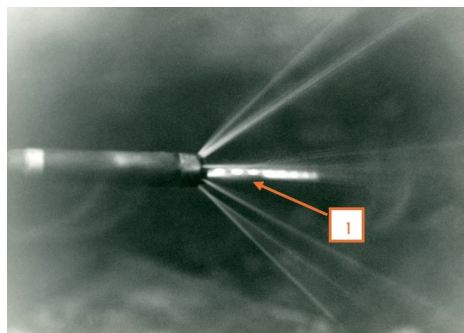
Fig.5. Spin detonation phenomenon of a supersonic high-temperature jet: 1 – spin detonation

Fig. 6 shows granite particles obtained by array processing with a thermal tool: G_{oxy} = 15 m^3/h, G_{ker}= 10 kg/h, P_{oxy}= 1.4 ÷ 1.5 MPa, d_{nt} = 4×10^{-3} m, α_{nt} = 0.8, T_g = 2780 K, W_g = 2410 m/s. For spraying the powder onto a metal substrate (stainless steel), the particles were selected by size: 0.1×10^{-3} m (2.9%); 0.25×10^{-3} m (3.8%); 0.5×10^{-3} m (7.1%) for spraying them in the form of powder on a heat exchange metal surface.
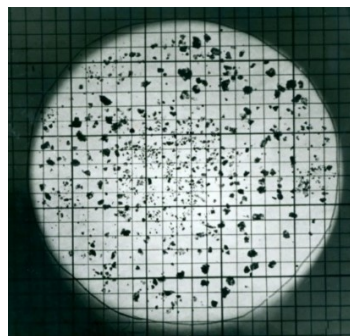
Fig.6. Granulometric composition of the «husk» obtained by processing Kurdai granite
with a kerosene-oxygen burner.

3.1. Method of fuel combustion

Afterburning of fuel (kerosene, gasoline) is performed on a barrier (coating). Oxidizer excess coefficient $\alpha < 1$, burner nozzle - shortened, combustion process - detonation. The afterburning process can be intensified up to two to six times. Maximum specific fluxes on the barrier: from (2 to 20)×10^6 W/m^2 (see Fig. 7). Application mode - without powder melting.
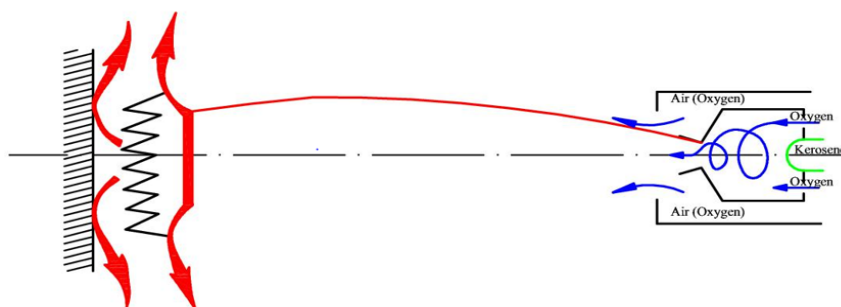
Fig.7. Detonation after-burning of fuel (kerosene) on the coating surface
made of natural material (granite) and a stainless-steel substrate.

The afterburning scheme was constructed by observing the process using optical methods (holography [23], laser LG-38 [6], and high-speed filming SKS-1M [24]). For the gas pressure in the burner combustion chamber of 0.5 MPa (on the coating the gas pressure will be approximately the same), the frequency of pressure fluctuation in the chamber is $\approx (500 \div 600)$ Hz, and on the coating (obstacle) is reduced to 200 Hz.

Control of the length of the burner jet flowing out of the nozzle. The dimensionless jet length $\bar{z} = \frac{z}{r_n}$ (see Table 1). For the maximum value of the heat transfer coefficient from the jet to the coating for one of the modes we take $\alpha_1 = 1000$ W/(m$^2\times$K).

Table 1. Dependence of α/α_1 on $\bar{z}$.

α/α_1	0.8	1	0.7	0.4	0.3
$\bar{z}$	0	10÷30	40	50	60

For $P_{c.c.} = 1$ MPa, $z = (0 \div 0.16)$ m, $T = (3500 \div 850)$ ^{0}C, $T_{st} = 3000$ ^{0}C – braking temperature (on the coating), $t_j = 300$ ^{0}C – temperature at the end of the free jet, $r_n = 3 \times 10^{-3}$ m, $r_j = 10 \times 10^{-3}$ m (jet radius).

Adjustment of the jet angle to the coating. In Table 2, the following is accepted: $\alpha_{90^0} = 1000$ W/(m$^2\times$K); $T_{st} = 3500$ ^{0}C; $t_j = 300$ ^{0}C; $P_{c.c.} = 1$ MPa.

Table 2. Dependence of α/α_{90^0} on $\bar{z}$.

α/α_{90^0}	1	1.1	1	0.8	0.5	0.35	0.3	0.25
β, deg.	90	80 – 75	60	50	30	20	10	0

Characteristics of thermal tools and parameters of sprayed powders of mineral media. Dependences of thermal loads for natural mineral media are presented in Fig. 8 and Fig. 9 for granite. Temporal dependences of ultimate thermal loads and thermomechanical stresses depending on particle size distribution were investigated by us in [24].
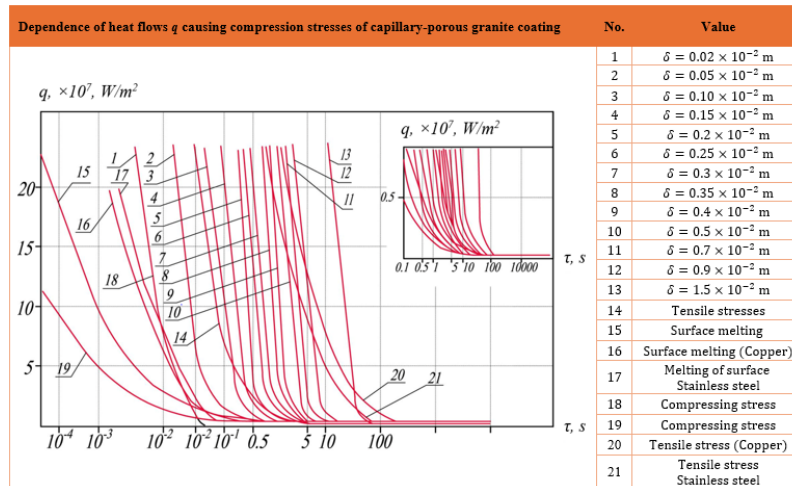
Fig.8. Limit ranges of thermal loads for granite coating

For the range of flight time of granite powder particles $\tau = (5 \div 9) \times 10^{-2}$ s, the thicknesses of coatings were in the interval - $\delta = (0.2 \div 0.5) \times 10^{-3}$ m, powder diameter - $d = (20 \div 100) \times 10^{-6}$ m. The ultimate tensile stresses, MPa, respectively for granite coatings were - 21. Fig. 9 shows the dependence $q = f(\delta, \tau)$, presented in Fig. 8, in the range $q = (0.25...0.75) \times 10^7$ W/m^2.

The dependences in Fig. 8, 9 have experimental confirmation [23]. The heat fluxes q of the burner jet were measured by a copper cylinder sensor, the process time τ and the size of the detached particle δ were measured by a high-speed movie camera SKS-1M [24]. The value of heat flows q can be reduced by one order when switching to another type of burner: benzo (kerosene) - air burners. Such burners are used for application of coating by spraying mineral medium with a lower strength value than that of granite, for example, teschenite, porphyrite or marble. The limiting ranges of thermal loads are presented in Section 4.
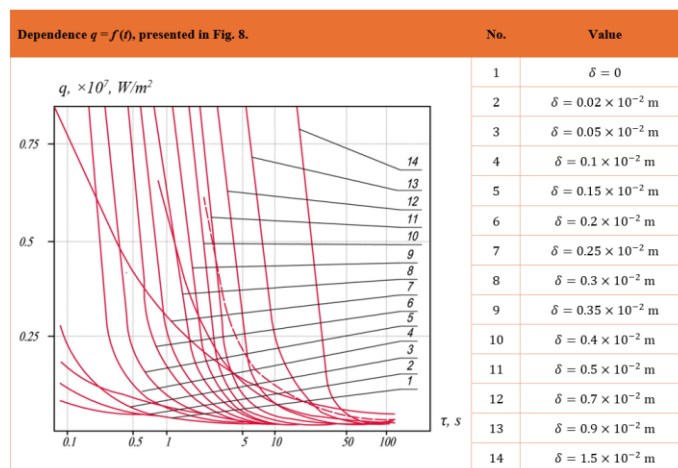
Fig.9. Limit ranges of thermal loads for granite coating $q = f(\delta, \tau)$.

3.2. Regulation of the power and type of burners.

For kerosene-oxygen burners of a thermal tool, we have the following characteristics: oxygen consumption G_{oxy} for pressure P_{oxy}= 1.2÷1.5 MPa, m³/h – 15÷18; kerosene consumption G_{ker} for pressure P_{ker} = 1.3÷1.5 MPa, kg/h – 10÷12; nozzle critical diameter is d_{nt}, 10^{-3} m – 4÷5; combustion chamber diameter is $d_{c.c.}$, 10^{-3} m – 14. Gas-dynamic parameters of jets at the outlet of the nozzle are summarized in Table 3.

Table 3. Gas-dynamic parameters of jets at the outlet of the nozzle.

α	$P_{c.c.}$ = 1.5 MPa	
	T_g, К	W_g, m/s
0.7	2670	2420
0.8	2780	2410
0.9	2830	2400
1	2810	2320

Fig. 10 shows the technique and technology of thermal tool operation with d_{nt} = (4÷5)×10^{-3} m, $d_{c.c.}$ = 14×10^{-3} m to granite impact surface. The flame structure, jet spreading radius (braking spot), the distance from the nozzle edge (outlet part) of the burner to the coating are visible. Removal of cooling water from the impact surface in the form of jets is carried out for technological reasons of applying a protective coating.


Fig. 10. Position of the torch to the granite processing surface, 1 - structure of the torch.

The protective shield is designed to protect the worker-operator of the thermal tool. Specific heat flows q on the coating surface were (5÷12) MW/m² for r = 0 and l = (4÷12)×10^{-2} m; (2÷5) MW/m² for r = 4×10^{-2} m and l = (4÷12)×10^{-2} m.

Distribution of q (r): q $(r) = q_{max} \times \exp(-1000 \times r^2)$, W/m^2. For a more powerful burner with $d_{nt} = 6 \times 10^{-3}$ m, $d_{c.c.} = 18 \times 10^{-3}$ m: G_{oxy} for $P_{oxy} = 1.8$ MPa, m^3/h – 30÷55; G_{ker} for $P_{ker} = (1.8\text{-}2)$ MPa, kg/h – 14÷18, we have q $(r = 0) = (6 \div 13)$ MW/m^2.

4. Comparison of the results with existing data on the theme

Let us make a comparative evaluation of the coatings studied in this work (see Fig. 11) with other cooling systems. The studied thermal characteristics of coatings made of natural material are related to high-intensity cooling systems. The comparison shows the advantages of boiling in bulk, thin films and in heat pipes.
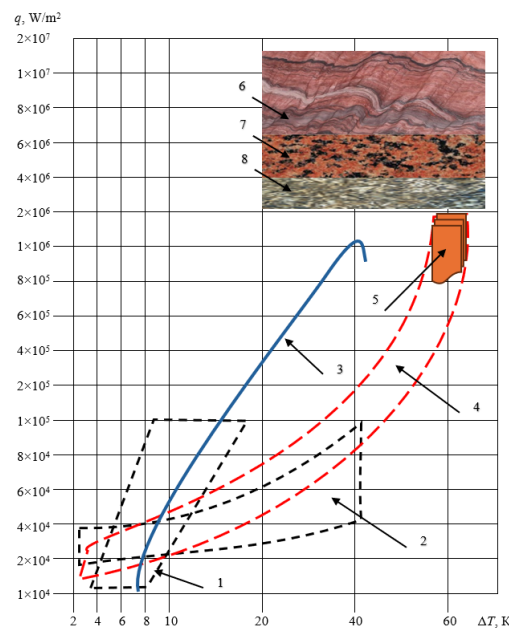
Fig. 11. Comparative evaluation of thermal load dependence on surface superheating

Fig. 11 shows the dependence of the thermal load on the wall superheat relative to the water vapor temperature (areas 1 - 4) (P = 0.1 MPa) [6], the designations in Fig. 11 are summarized in Table 4. As can be seen from Fig. 11, high $q_{cr.}$ are achieved in the case of the jet coolant supply, since in the jet braking zone there is high turbulence (intense pulsations), very thin boundary layer, negative pressure gradient dP/dx and active vapor film collapse.

Table 4. Comparative evaluation.

No. Area	Denomination	References to the authors' comparative scientific papers
1	Scope of work of thin-film evaporators	[11].
2	Scope of work of heat pipes with mesh wicks	[10], [12], [13], [14].
3	High-volume boiling on uncoated surfaces	[12], [13], [14], [15], [16], [17], [18], [19].
4	Researched mesh capillary-porous cooling system	[6].
5	Shaded area - application of intensifiers in a porous system	[24].
6	Thermal load limit areas for natural mineral medium with no surface melting for quartz coatings	[23].
7	Thermal load limit areas for natural mineral medium with no surface melting for granite coatings	See Fig. 8 and Fig. 9.
8	Thermal load limit areas for natural mineral medium with no surface melting for teschenite coatings	[26].

The thermal protection of CPCs (capillary porous coatings) is improved due to structural temperature gradients. Synthesis of powders of mineral media produced in the foci of elliptical cylinders, or due to impact processes and structural detonation, gives undeniable advantages in the creation of coatings with

gradient nanostructure. Such materials have high mechanical properties, combining the synergistic advantages of strength and plasticity, strain hardening, increased resistance to cracking, fracture and fatigue. Structural thermal gradients create thermal stress and strain gradients.

5. A model of interaction of an axisymmetric supersonic detonation jet of gases of a thermal instrument according to standards with the surface of a capillary-porous coating

Let us consider the interaction of the supersonic jet of the thermal tool (see Fig. 5 and Fig. 7) with the obstacle in the braking zone (the vicinity of the critical point) (see Fig. 10). The jet is located orthogonally (perpendicularly) to the coating surface. Let us write down for «standard conditions» the heat transfer equation [25] in the laminar boundary layer in the longitudinal flow of the plate:

$$Nu_x = K_1\sqrt{Re_x}\sqrt[3]{Pr} , \tag{1}$$

where $Re_x = W_\infty \cdot \frac{x}{\nu}$, $W_\infty = W_0$. Local heat transfer during longitudinal flow around the plate in a turbulent boundary layer [26]:

$$Nu_x = K_2 \cdot Re_x^{0.8} \cdot Pr^{0.43}, \tag{2}$$

where $T_{st} = const$; $10^5 < Re_x < 10^7$. In the formula (1) $K_1 = 0.323$; in the formula (2) $K_2 = 0.0296$.

The thermo-physical properties of gas are assumed at an average temperature between T_∞ and T_{st}; more often in models, the temperature of the undisturbed flow T_∞, or T_{st} is selected as the determining temperature;

$Pr = \frac{\nu}{\alpha}$ – Prandtl number; Nu_x – Nusselt number;

$Nu_x = \alpha_x \cdot \frac{x}{\lambda}$.

Let us rewrite the number Nu_x and the criterion Re_x in a form which is more convenient for analysis.

The Reynolds Criterion:

$Re_x = \frac{\rho_0 \cdot W_0 \cdot x}{\mu_x}$.

The Nusselt number:

$Nu_x = \frac{q(x) \cdot x}{\lambda_x \cdot (Ta_{st} - T_{st})}$,

Then we calculate the temperature Ta_{st}:

$$Ta_{st} = Tr_\infty, \text{K}, \tag{3}$$

where Tr_∞ is the recovery temperature equal to:

$$Tr_\infty = T'_\infty + r \cdot \frac{W_\infty^2}{2cp_\infty}, \text{K}; \tag{4}$$

T'_∞ – the thermodynamic temperature of an undisturbed flow (this is the temperature that a thermometer moving with the flow at the same speed with it would show). For $Pr = 1$:

$$T_{0\infty} = T'_\infty + r \cdot \frac{W_\infty^2}{2cp_\infty}, \text{K}, \tag{5}$$

Ta_{st} – the temperature of the coating itself or the adiabatic temperature of the wall (the temperature of an ideally insulated, non-radiating solid surface, streamlined by a gas flow with internal heat sources or with the release of heat due to energy dissipation). When $Pr < 1$, $Ta_{st} < T_{0\infty}$.

Recovery factor:

$$r = \frac{Ta_{st} - T'_\infty}{T_{0\infty} - T'_\infty} . \tag{6}$$

For laminar layers:

$$r = \sqrt{Pr}. \tag{7}$$

The thermodynamic temperature is T'_∞ equal to:

$$T'_\infty = \frac{\alpha_\infty^2}{K \cdot R}, \text{K}. \tag{8}$$

Braking temperature:

$$T_{0\infty} = T_\infty \cdot \left[1 + \frac{(K-1)}{2} \cdot M_\infty^2\right], \text{K}. \tag{9}$$

The recovery temperature is equal to:

$$T_{r\infty} = T_\infty \cdot \left[1 + r \cdot \frac{(K-1)}{2} \cdot M_\infty^2\right], \text{K}, \tag{10}$$

where $K = \frac{Cp}{C\vartheta}$.

5.1. Calculation of specific heat flows q_{st}

The heat flow of the gas streamlined by the high-speed flow is defined as:
$$q_{st} = \alpha \cdot (Ta_{st} - T_{st}), \text{ W/m}^2. \tag{11}$$
If $\neq 1$, then
$$Ta_{st} = T_{r\infty}, \tag{12}$$
and $q_{st} = \alpha \cdot (T_{r\infty} - T_{st})$, W/m^2.
If $= 1$, then
$$Ta_{st} = T_{0\infty}, \tag{13}$$
and $q_{st} = \alpha \cdot (T_{0\infty} - T_{st})$, W/m^2.

For a detonation supersonic flame, we conducted experiments using a micro-nozzle for measuring total and static pressures and a heat flow sensor for measuring $q(x)$, α_x, M_x and $\rho_0 W_0$ in a spraying jet. Mach numbers $M = \frac{W_g}{\alpha} = 2.3$. The degree of non-calculation of outflow $n_a = \frac{P_e}{P_b} = 0.8$. The number Re_a was calculated based on the parameters of the gas at the nozzle edge (index «a»):
$$Re_a = \frac{W_a \cdot d_a}{\nu_a}, \text{ where } Re = 1\times10^6; \bar{l} = \frac{l}{d_a} = 3.$$

When a supersonic jet of the thermal tool interacts with an obstacle in the deceleration zone (near the critical point), a combined effect takes place: high turbulence intensity, negative pressure gradient, and wave structures that generate turbulence (pulsations), causing flow separation from the wall. Such a jet belongs to the impact type and affects the mechanism of heat transfer at the stagnation point of the coating. It increases turbulence (pulsations), and in the case of a boiling cooling system, destroys vapor conglomerates.

In the vicinity of the critical point (on the coating), a laminar flow regime is assumed, since the Reynolds number Re_x is not high and a negative pressure gradient is present. However, the Nusselt number Nu_x is found to be 5–6 times higher than that predicted by laminar theory (formula (1)). This may indicate a detonation effect of turbulent pulsations penetrating the laminar boundary layer from the outer flow. At $Re_x \geq 4\times10^5$, the points lie below the curve corresponding to the turbulent boundary layer ($10^5 < Re_x < 10^7$) for subsonic flows.

Thus, for the «standard conditions» of heat exchange, K$_1$ = 0.323 and K$_2$ = 0.0296. In case of a detonation supersonic wave, we have for $Re_x < 4\times10^5$, $K_1' = (5\div6)\times K_1$ and for $10^6 \geq Re_x \geq 4\times10^5$, $K_2' = 0.95\times K_2$.

6. Conclusions

1. Effective coating deposition from various natural materials is achieved through the use of a detonation burner. The main coating parameters have been determined.

2. The cooling system demonstrated high efficiency up to the critical state of the combustion chamber metals and nozzles.

3. A model was developed for the interaction of an axisymmetric supersonic detonation gas jet of the thermal tool acting normally to the coating. The experimentally obtained heat transfer coefficients were found to be 5-6 times higher than those predicted by laminar theory and several times lower than those predicted by turbulent heat transfer laws.

4. The developed surfaces in the form of coatings and mesh structures provide a positive effect due to the advantages of combined manufacturing technologies, enabling an increase in dissipated thermal loads.

5. A comparative evaluation of the coatings demonstrated their advantages over traditional cooling systems.

References

1   Wei Chen, Wuwen Liu, Yue Liang. (2024) An Investigation into the Compressive Strength, Permeability and Microstructure of Quartzite-Rock-Sand Mortar. *Fluid Dynamics and Materials Processing*, 20(4), 859-872. https://doi.org/10.32604/fdmp.2023.029310

2   Ramadji C., Messan A., Prud'Homme E. (2020) Influence of Granite Powder on Physico-Mechanical and Durability Properties of Mortar. *Materials,* 13, 5406. https://doi.org/10.3390/ma13235406

3   Ju Wang, Feng Dai, Yi Liu, Hao Tan, Pan Zhou. (2024) Thermophysical-mechanical behaviors of hot dry granite subjected to thermal shock cycles and dynamic loadings. *Journal of Rock Mechanics and Geotechnical Engineering,* https://doi.org/10.1016/j.jrmge.2024.09.007

4   Ting Zuo, Xianglong Li, Jianguo Wang, Qiwen Hu, Zihao Tao, Tao Hu. (2024) Insights into natural tuff as a building material: Effects of natural joints on fracture fractal characteristics and energy evolution of rocks under impact load. *Engineering Failure Analysis*, 163(Part A), 108584. https://doi.org/10.1016/j.engfailanal.2024.108584

5   Yan Zhang, Chunchi Ma, Yaohui Gao, Kai Meng. (2024) Investigation on mechanical behaviors and energy characteristics of deep-buried marble in a hydraulic tunnel in Southwest China. *Transportation Geotechnics*, 47, 101270. https://doi.org/10.1016/j.trgeo.2024.101270

6   Genbach A., Beloev H., Bondartsev D. (2021) Comparison of cooling systems in power plant units. *Energies,* 14, 6365. https://doi.org/10.3390/en14196365

7   Shavdinova M.D., Sharipov R.Zh., Meshherjakova T.Y. (2021) Enhancement of steam-turbine condenser steam-jet ejector. *Eurasian Physical Technical Journal,* 18, 4(38), 52-58. https://doi.org/10.31489/2021No4/52-58

8   Komarov I.I., Vegera A.N., Bryzgunov P.A., Makhmutov B.A., Smirnov A.O. (2022) Development and research of the topology of cooling baffles for blades of the axial carbon dioxide turbines. *Eurasian Physical Technical Journal*, 19, 2(40), 48-57. https://doi.org/10.31489/2022No2/48-57

9   Zlateva P., Terziev A., Murzova M., Mileva N., Vassilev M. (2025) Market Research on Waste Biomass Material for Combined Energy Production in Bulgaria: A Path Toward Enhanced Energy Efficiency. *Energies,* 18(15), 4153. https://doi.org/10.3390/en18154153

10   Riadh Boubaker, Vincent Platel. (2016) Dynamic model of capillary pumped loop with unsaturated porous wick for terrestrial application. *Energy*, 111, 402-413. https://doi.org/10.1016/j.energy.2016.05.102

11   Jamialahmadi M., Müller-Steinhagen H., Abdollahi H., Shariati A. (2008) Experimental and theoretical studies on subcooled flow boiling of pure liquids and multicomponent mixtures. *International Journal of Heat and Mass Transfer*, 51(9-10), 2482-2493. https://doi.org/10.1016/j.ijheatmasstransfer.2007.07.052

12   Mieczyslaw E. Poniewski. (2004) Peculiarities of boiling heat transfer on capillary-porous coverings. *International Journal of Thermal Sciences*, 43(5), 431-442. https://doi.org/10.1016/j.ijthermalsci.2003.10.002

13   Kimihide Odagiri, Hosei Nagano. (2019) Investigation on liquid-vapor interface behavior in capillary evaporator for high heat flux loop heat pipe. *International Journal of Thermal Sciences*, 140, 530-538. https://doi.org/10.1016/j.ijthermalsci.2019.03.008

14   Ji X., Xu J., Zhao Z., Yang W. (2013) Pool boiling heat transfer on uniform and non-uniform porous coating surfaces. *Experimental Thermal and Fluid Science*, 48, 198-212. https://doi.org/10.1016/j.expthermflusci.2013.03.002

15   Mohammad S.A., Prasad L., Gupta S.C., Agarwal V.K. (2008) Enhanced boiling of saturated water on copper coated heating tubes. *Chemical Engineering and Processing: Process Intensification*, 47(1), 159-167. https://doi.org/10.1016/j.cep.2007.07.021

16   Chen Li, Peterson G.P., Yaxiong Wang (2006) Evaporation/Boiling in Thin Capillary Wicks (l) - Wick Thickness Effects. *Journal of Heat Transfer*, 128(12), 1312-1319. https://doi.org/10.1115/1.2349507

17   Hanlon M.A., Ma H.B. (2003) Evaporation Heat Transfer in Sintered Porous Media. *Journal of Heat Transfer*, 125(4), 644-652. https://doi.org/10.1115/1.1560145

18   Chen Li, Peterson G.P. (2006) Evaporation/Boiling in Thin Capillary Wicks (II) - Effects of Volumetric Porosity and Mesh Size. *Journal of Heat Transfer*, 128(12), 1320-1328. https://doi.org/10.1115/1.2349508

19   Das A.K., Das P.K., Saha P. (2009) Performance of different structured surfaces in nucleate pool boiling. *Applied Thermal Engineering*, 29(17-18), 3643-3653. https://doi.org/10.1016/j.applthermaleng.2009.06.020

20   Mehmet Arik, Avram Bar-Cohen, Seung Mun You. (2007) Enhancement of pool boiling critical heat flux in dielectric liquids by microporous coatings. *International Journal of Heat and Mass Transfer*, 50(5-6), 997-1009. https://doi.org/10.1016/j.ijheatmasstransfer.2006.08.005

21   Mohammad S.S., Yong H.J., Soon H.C. (2007) Subcooled flow boiling CHF enhancement with porous surface coatings. *International Journal of Heat and Mass Transfer*, 50(17-18), 3649-3657. https://doi.org/10.1016/j.ijheatmasstransfer.2006.09.011

22   Forrest E., Williamson E., Buongiorno J., Hu L., Rubner M., Cohen R. (2010) Augmentation of nucleate boiling heat transfer and critical heat flux using nanoparticle thin-film coatings. *International Journal of Heat and Mass Transfer*, 53(1-3), 58-67. https://doi.org/10.1016/j.ijheatmasstransfer.2009.10.008

23   Genbach A.A., Bondartsev D.Y. (2020) Limiting Thermal State of Capillary-Porous Power-Plant Components. *Russian Engineering Research*, 40, 384-389. https://doi.org/10.3103/S1068798X20050093

24   Genbach A.A., Bondartsev D.Y., Iliev I.K. (2018) Modelling of capillary coatings and heat exchange surfaces of elements of thermal power plants. *Bulgarian Chemical Communications*, 50(G), 133-139. Available at: https://www.researchgate.net/profile/Iliya-Iliev-2/publication/330385900_Modelling_of_capillary_coatings_and_heat _exchange_surfaces_of_elements_of_thermal_power_plants/links/5c3dcf32458515a4c727ef12/Modelling-of-capillary-coatings-and-heat-exchange-surfaces-of-elements-of-thermal-power-plants.pdf

25   Kutateladze (1990) Heat transfer, mass transfer, and friction in turbulent boundary layers. *Hemisphere*, 367. https://discovery.hw.ac.uk/permalink/f/i526e0/44hwa_alma2127993300003206 [in Russian]

26   Genbatch A.A., Bondartsev D.Y. (2018) Experimental method of investigation of the heat transfer crisis in a capillary-porous cooling system. *News ofthe National Academy of Sciences of the Republic of Kazakhstan-Series of Geology and Technical Sciences,* (2), 81-88. Available at: http://www.geolog-technical.kz/images/pdf/g20182/229-235.pdf [in Russian]

_____

AUTHORS' INFORMATION

Genbach, Aleksandr A. — Doctor of Science (Eng.), Professor, Professor, Department of Heat Power Engineering, Institute of Energy and Green Technologies, Almaty University of Power Engineering and Telecommunications named after G. Daukeev; Scopus Author ID: 6603206395; https://orcid.org/0009-0001-3819-4387, a.genbach@aues.kz

Bondartsev, David Yu. — Doctor of Philosophy (PhD), Associate Professor, Professor, Department of Heat Power Engineering, Institute of Energy and Green Technologies, Almaty University of Power Engineering and Telecommunications named after G. Daukeev; WoS Researcher ID: AFD-9189-2022, Scopus Author ID: 57202869716; https://orcid.org/0000-0001-8778-7851, d.bondartsev@aues.kz